Sensors and Actuators A 317 (2021) 112373

Contents lists available at ScienceDirect

Sensors and Actuators A: Physical

journal homepage: www.elsevier.com/locate/sna

Photosensitive activity of fabricated core-shell composite nanostructured p-CuO@CuS/n-Si diode for photodetection applications

S. Gunasekaran[a], D. Thangaraju[b,*], R. Marnadu[c], J. Chandrasekaran[c], Mohd. Shkir[d,e], A. Durairajan[f], M.A. Valente[f], T. Alshaharani[g], M. Elango[a,*]

[a] Department of Physics, PSG College of Arts and Science, Coimbatore, 641014, Tamil Nadu, India
[b] Nano-Crystal Design and Application Lab (NCDAL), Department of Physics, PSG Institute of Technology and Applied Research, Coimbatore, 641062, Tamil Nadu, India
[c] Department of Physics, Sri Ramakrishna Mission Vidyalaya College of Arts and Science, Coimbatore, 641 020, Tamil Nadu, India
[d] Research Center for Advanced Materials Science (RCAMS), King Khalid University, P.O. Box 9004, Abha, 61413, Saudi Arabia
[e] Advanced Functional Materials and Optoelectronics Laboratory (AFMOL), Department of Physics, College of Science, King Khalid University, Abha, 61413, Saudi Arabia
[f] I3NAveiro, Department of Physics, University of Aveiro, 3810 193, Aveiro, Portugal
[g] Department of Physics College of Science Princess Nourah Bint Abdulrahman University Riyadh 11671 Saudi Arabia

ARTICLE INFO

Article history:
Received 13 July 2020
Received in revised form
14 September 2020
Accepted 7 October 2020
Available online 14 October 2020

Keywords:
CuS@CuO
Core/shell heterostructure
Photoresponse
Photodetector

ABSTRACT

Development of photo detectors based on different semiconducting materials with high performance has been in progress in recent past, however, there is a lot of difficulties in developing the more effective photo detectors-based devices with high responsivity, detectivity and quantum efficiency. Hence, we have synthesized pure CuS and CuO@CuS core-shell heterostructure based photo detectors with high performance by simple and cost-effective two-step chemical co-precipitation method. The phase purity of CuS and CuO@CuS composite was observed by XRD analysis and the result were verified with Raman spectroscopy studies. Sphere like morphology of pure CuS and core-shell structure formation of CuO@CuS are observed with scanning and transmission electron microscopes. The presence of expected elements has been confirmed with EDX elemental mapping. Light harvesting photodiodes were fabricated by using n-type silicon substrate through drop cost method. Photo sensitive parameters of fabricated diodes were analyzed by I–V characteristics. The p-CuO@CuS (1:1)/n-Si diode owned a maximum photosensitivity (Ps) ~ 7.76×10^4 %, photoresponsivity (R) ~ 798.61 mA/W, external quantum efficiency (EQE)~309.66 % and specific detectivity (D*) ~ 8.19×10^{11} Jones when compared to p-CuS/n-Si diode. The obtained results revealed that the core/shell heterostructure of CuO@CuS is the most appropriate for photo detection.

1. Introduction

Incorporating novel structure in photo detector is an important task to enhance the opto-electrical performance of the devices. Recently, hybrid nanomaterials and its structural, morphological, and electrical properties are drawn much attention in fabrication of devices such as solar cell, photo detectors, and super capacitors [1]. Many transition metal oxide (TMO) and transition metal chalcogenide (TMC) nanomaterials are well-known semiconducting materials, which are widely used for construction of optoelectronic devices due to its potential light absorbing nature. The generation of charge carriers and the charge carrier transport mechanism of TMO and TMC nanomaterials are most favorable for photo sensitive device fabrication [2]. In previous reports TMO (MoO_3, WO_3, and CuO) and TMC (ZnS, MoS_2, WS_2 and CuS) based photo detectors and are widely studied in terms of effect of morphology, concentration and temperature [3–6].

The heterostructure in optoelectronic application will improve the light abortion rate of the junction and it has strong current carrying nature. The heterojunction with different material with same conducting nature will improve the photo sensing nature of the device. Particular interest, the development of core/shell heterostructure are attractive towards the photo detectors because of

* Corresponding author.
E-mail addresses: thangaraju@psgitech.ac.in (D. Thangaraju), elango@psgcas.ac.in (M. Elango).

https://doi.org/10.1016/j.sna.2020.112373
0924-4247/

their surface to volume ratio, which enable high photo response and charge transport mechanism without any loss of charge carriers [7]. Photo sensitive parameters were effectively influenced by incorporating the core/shell based sensitive layer which reduce the width of the depletion layer, barrier height, and increase the free carrier charge transport [8].

Recently many researchers reported that the fabrication and characterization of photo detectors using the core/shell nanostructures with the composition of organic/inorganic material with different nanostructures [9–11]. Zheng Sun et al. reported that highly sensitive photo detectors based on Ge–CdS core–shell heterojunction nanowires which show better photo response [12]. Improved photo response and carrier transport mechanism of ZnO/graphene core-shell structure-based photo detector was reported by Shao et al. [13]. In recent past CuO & CuS based core-shell photodetectors has been developed by several scientists like the p-CuO/n-MoS_2 flexible heterojunction photo detector was reported by Zhang et al. with low-dark current ~ 0.039 nA and highest detectivity ~ 3.27×10^8 Jones [14], Xie et al. developed the nanostructured p-CuO/n-ZnO heterojunction photodetector and observed the responsivity ~ 0.040A/W at 1 V and 0.123 A/W at 2 V, Xie et al. reported the CuO/SnO_2 UV photodetector and noticed the enhancement [15], Tian et al. fabricated the $In_2Ge_2O_7$ photodetector with CuO coating and observed the high responsivity and quantum efficiency ~ 7.34×10^5 A W^{-1} & 3.5×10^6, respectively [16], Sahatiya et al. reported the MoS_2(n)–CuO(p) flexible diode on cellulose paper with ideality factor 1.89 eV, barrier height 0.243 eV, and responsivity ~ 42 mA/W [17], Shin et al. developed the p-CuO/n-$Cu_{1-x}In_xO$ core/shell UV photodetector and noticed the photoresponsivity ~ 0.045 A/W [18], CuO/ZnO based UV photodetector with improved electrical nature was developed by Noothongkaew et al. [19], UV detector based on ZnO/CuO was fabricated with by Vikas et al. [20], Mohammadi et al. reported the ZnO/NiO(CuO) photodetector with enhanced properties [21], p-CuO/n-ZnO photodetectors has been fabricated by Ji et al. [22]. Xu et al. p-CuS-ZnS/n-ZnO photodetectors with responsivity ~ 12 mA W^{-1} at 300 nm [23], Zhnag et al. developed the n-$SrTiO_3$ (n-STO) and p-CuS-ZnS (p-CZS) photodetectors with highest responsivity ~ 5.4 μA W^{-1} (at 390 nm), detectivity ~ 1.6×10^9 Jones [24], Panigrahi et al. fabricated n-ZnO/p-CuS photodetectors and investigated [25], etc. Along with the above-mentioned materials there are several other materials who has been employed and investigated as UV photodetectors like: $Sr_2Nb_3O_{10}$ with R = 1214 A W^{-1}, EQE = 5.6×10^5 %, D* = 1.4×10^{14} Jones @270 nm and 1 V bias by Li et al. [26], and several other 2D photodetectors (BP, GaSe, MoS_2 and SnSe) discussed by Zhang et al. [27], $BaTiO_3/MoS_2$ reported by Ying et al. with R_λ of 120 vs 1.7 A W^{-1} & EQE of 4.78×10^4 vs 4.5×10^2% @365 nm compare to bare MoS_2 [28], and Li et al. reported the hybrid CuO@In_2O_3 with R = 2.24×10^4 A/W [29]. These studies are showing very high values compare to current results; however, the currently developed photodetector is the first-time report to the literature and further work is in progress to achieve higher photodetection properties by varying the several preparation parameters. As the core/shell combinations of TMO and TMC are expected to enhance the photocurrent and responsivity of the photo detector. Most of the core/shell heterojunction-based photodiodes was reported on p-type or n-type material, still efficiency in Photo response is lagging, to achieve better photo response both material for the heterojunction employed as p-type semiconducting material [30].

These reports indicate that the core-shell system based on CuO & CuS both possess highly improved photodetection properties which makes it more useful in nanoelectronics devices with fascinating functions. Also, among several materials CuO & CuS are a versatile p-type semiconducting material with extensive properties such as earth abundance, mechanical stability, narrow band gab, cost effective, are increasing attention in the fabrication of photo detector [31,32]. Till date the CuS with CuO as core/shell heterojunction is not documented. So, in this report, synthesis of pure CuS and CuS@CuO core/shell nanocomposite was done by the two-step co-precipitation method. The photo response properties of fabricated photodiodes such as p-CuS/n-Si and p-CuO@CuS-n/Si are explored in detail.

2. Materials and method

2.1. Materials

Copper (II) chloride dihydrate (98.5 %, $CuCl_2.2H_2O$), Thiourea (99 %, CH_4N_2S), Ammonia Solution (assay 25 %, NH_3OH) were procured from Merck Life Sciences. All the chemicals used in this work are used as purchased.

2.2. Preparation of CuS nanoparticle

The synthesis of CuS was carried out through co-precipitation method. $CuCl_2.2H_2O$ (5 mmol) was dissolved in 80 mL of distilled water and CH_4N_2S (10 mmole) was added. The solution was subjected to vigorous stirring about 30 min at room temperature. The solution was adjusted to pH 10 using NaOH solution at 60 °C. The above solution was stirred for 2 h and formed precipitate was centrifuged (3000 rpm for 10 min) and collected. Obtained precipitate was washed about three times using distilled water and ethanol. The precipitate was dried at 50 °C in hot air oven and stored for further characterization.

2.3. Fabrication of CuO nanoparticles

Pure CuO nanoparticles were co-precipitationally achieved. In this method, 0.2 mol of $CuCl_2.2H_2O$ dissolved in 100 mL distilled water and stirred for 30 min to get homogenous green solution. The pH of above solution was adjusted to pH 9 using NH_4OH solution. The color of the solution turned in to black, when the solution attained pH 9. The collection of the precipitate was done after centrifuging at 3000 rpm for 5 min and washing with ethanol and distilled water.

2.4. Preparation of CuO@CuS nanocomposite

The core-shell CuO@CuS (1:0.5) prepared through by two-step chemical co-precipitation method. Previously prepared 0.440 *g* of CuO was completely dispersed in 80 mL of distilled water and stirred for 10 min after that 2.5mmole of $CuCl_2$ $2H_2O$was added as a copper source and stirred about 20 min for homogeneous dispersion. Thiourea (5 mmole) is added as a sulfur source after a continuous stirring about 30 min the solution changed from greenish to navy blue color. pH of the Solution was adjusted to 9 at 60 °C and stirred for 2 h. Formed precipitate was centrifuged at 3000 rpm and washed several times with distilled water and ethanol. The procedure was repeated for CuO@CuS (1:1) as mentioned above except Cu (5 mmole) and sulfur source (10 mmole).

2.5. Photodiode fabrication

The photodiodes are constructed by using one side polished n-Si substrate (1 × 1). Before starts the coating process the substrate was well cleaned to remove dust particle, oil and grease, organic/inorganic impurities, and native oxide layer over the surface of Si substrate. Substrates are immersed in 2 mL of iso-propanol and ultrasonicate for 5 min to remove the dust particle, then it transferred to another beaker which contains acetone in order to remove the oil and grease on the substrate. Next step in the cleaning

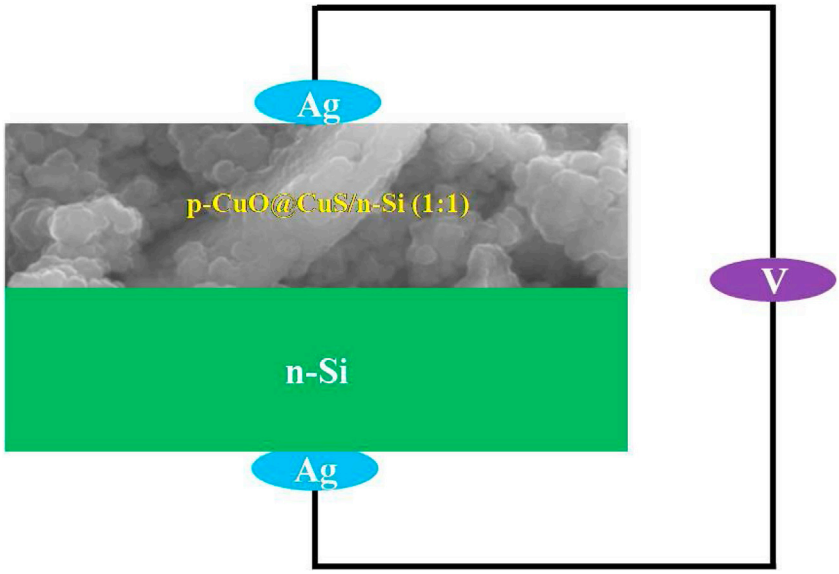

Fig. 1. Schematic diagram of p-CuO@CuS(1:1)/n-Sidiode.

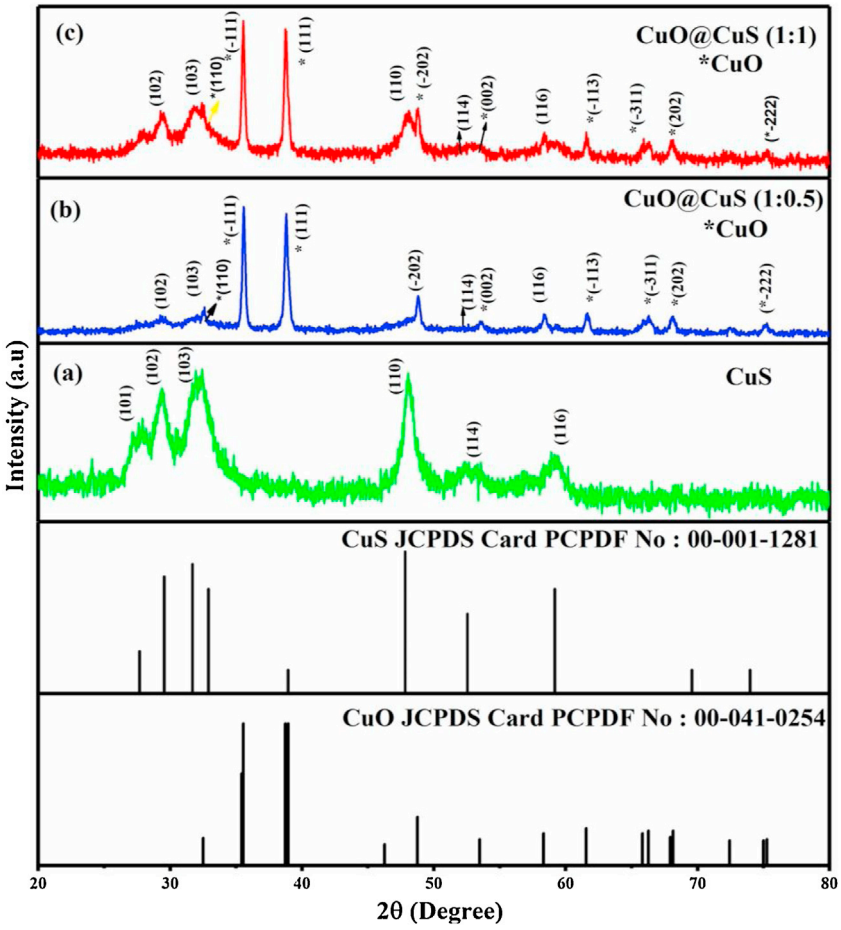

Fig. 2. Comparative XRD graph of for (a) CuS, (b) CuO@CuS (1:0.5), (c) CuO@CuS(1:1).

process, substrate was cleaned using piranha solution (H_2SO_4-H_2O_2) (2:1) to eliminate inorganic/organic residues on Si substrate. Finally, substrates were immersed in (HF: H_2O) solution (1:10 ratio) for 10 min after that washed with DI water to eradicate the native SiO_2 layer [33]. As synthesized (50 mg) nanoparticle were dispersed in solution of cyclohexane (1 mL) and oleylamine (20 μL) to form ink type coating solution. Prepared pure CuS, CuO@CuS(1:0.5) and CuO@CuS(1:1) ink was coated on the n-Si substrate by drop cost method. The n-Si substrate was dried in room temperature about 1 h further annealed at 220 °C for one hour under N_2 atmosphere after coating a desired layer. An adhesive silver paste was applied on both sides to make the better contact and dried at ambient tem-

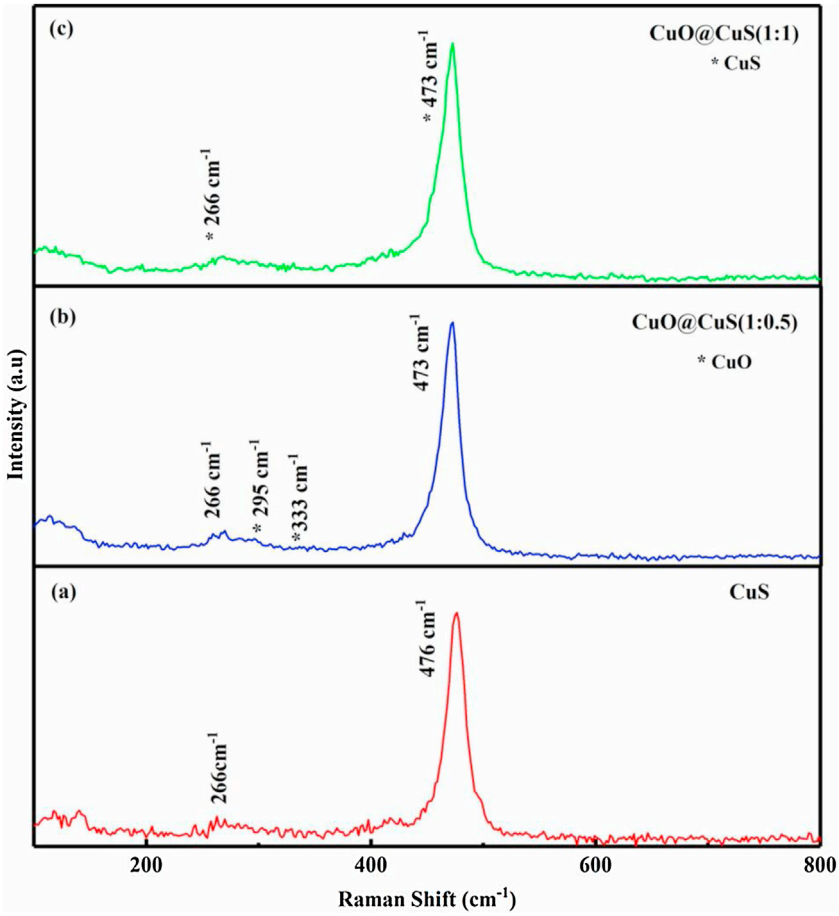

Fig. 3. Comparative graph of Raman for (a) CuS, (b) CuO@CuS (1:0.5), (c) CuO@CuS(1:1).

perature about 5 h. Schematic diagram of diode fabrication was presented in Fig. 1.

2.6. Material characterization methods

Structural analysis of synthesized CuS and CuO@CuS were performed by Philips PAN alytical Xpert pro powder X-ray diffractometer equipped with CuK_α radiation source of 1.54 Å. Raman spectra of the synthesized samples were recorded by Jobin Yvon HR 800 spectrometer with 532 nm laser sources. Morphology and elemental combination were analyzed using S-3400 N Hitachi field emission scanning electron microscope (FESEM). The morphology of CuO@CuS (1:1) core/shell structure was recorded by JEOL-JEM transmission electron microscopy (TEM) (model: 2100-Japan) at the accelerating voltage of 200 kV with SEAD pattern. The current-voltage characteristics were performed by Keithley source analyzer (6517-B) and the dark and photocurrent were measured with transferrable solar simulator (PEC-L01). The optimized white light with intensity of 100 mW/cm^2 was used for the diode parameter measurement.

3. Results and discussion

3.1. Structural & optical analyses

The XRD pattern obtained for pure CuO, CuO@ CuS (1:0.5) and CuO@CuS (1:1) are compared in Fig. 2. Obtained XRD pattern of CuS nanoparticle (Fig. 2 (a)) was well matched with standard hexagonal CuS structure (JCPDS card No: 00-001-1281) space group P63/mmc and cell parameters (a = 3.8020 b = 16.4300). CuO@CuS (1:0.5) and CuO@CuS (1:1) formation were agreed to usual hexagonal CuS and monoclinic CuO systems (JCPDS card no 00-041-0254; space group C2/c and a = 4.6850, b = 3.4230, and c = 5.1320 cell parameters). The broad and sharp reflection patterns were observed for CuS and CuO, respectively, which indicates the major size difference between core and shell particles [1,34]. No impurities from the other phases incorporated in the specimen are observed.

The optical absorption spectra of CuS, core-shell CuO@ CuS (1:0.5) and CuO@CuS (1:1) specimens were recorded as displayed in Fig. S1 (see supporting data). The band gap values were determined through Kubelka-Munk theory and the plots are presented in Fig. S2(see supporting data). The E_g values for CuS, CuO@ CuS (1:0.5) & CuO@CuS (1:1) were noted ~ 2.07, 1.91 and 1.88 eV, respectively.

3.2. Raman analysis

The Raman spectrum of the CuS, core-shell CuO@ CuS (1:0.5) and CuO@CuS (1:1) nanoparticle were compared in Fig. 3 (a–c). An intense peak observed around ~ 474 cm^{-1} and a tiny peak ~ 266 cm^{-1} in Fig. 3(a) are assigned to characteristic vibrational modes present in covellite CuS and the strong peak at ~ 476 cm^{-1} confirm the formation of covalite CuS formation which represents SS—stretching vibration mode of S_2 ions at 4e sites [35]. This result is well matched with Adhikar et al. and Kundu et al. and aligned in periodic array atom was revealed [36–38]. A tiny shoulder peak observed in the spectra at ~266 cm^{-1} is arising from the A_{1g} vibration bond of Cu-S [39]. Fig. 3(b) shows the Raman spectra of core shell CuO@CuS (1:0.5) nanocomposite exhibits both the characteristic Raman vibrational modes of CuO and CuS respectively. These results are good agreement with XRD results. In this spectrum two

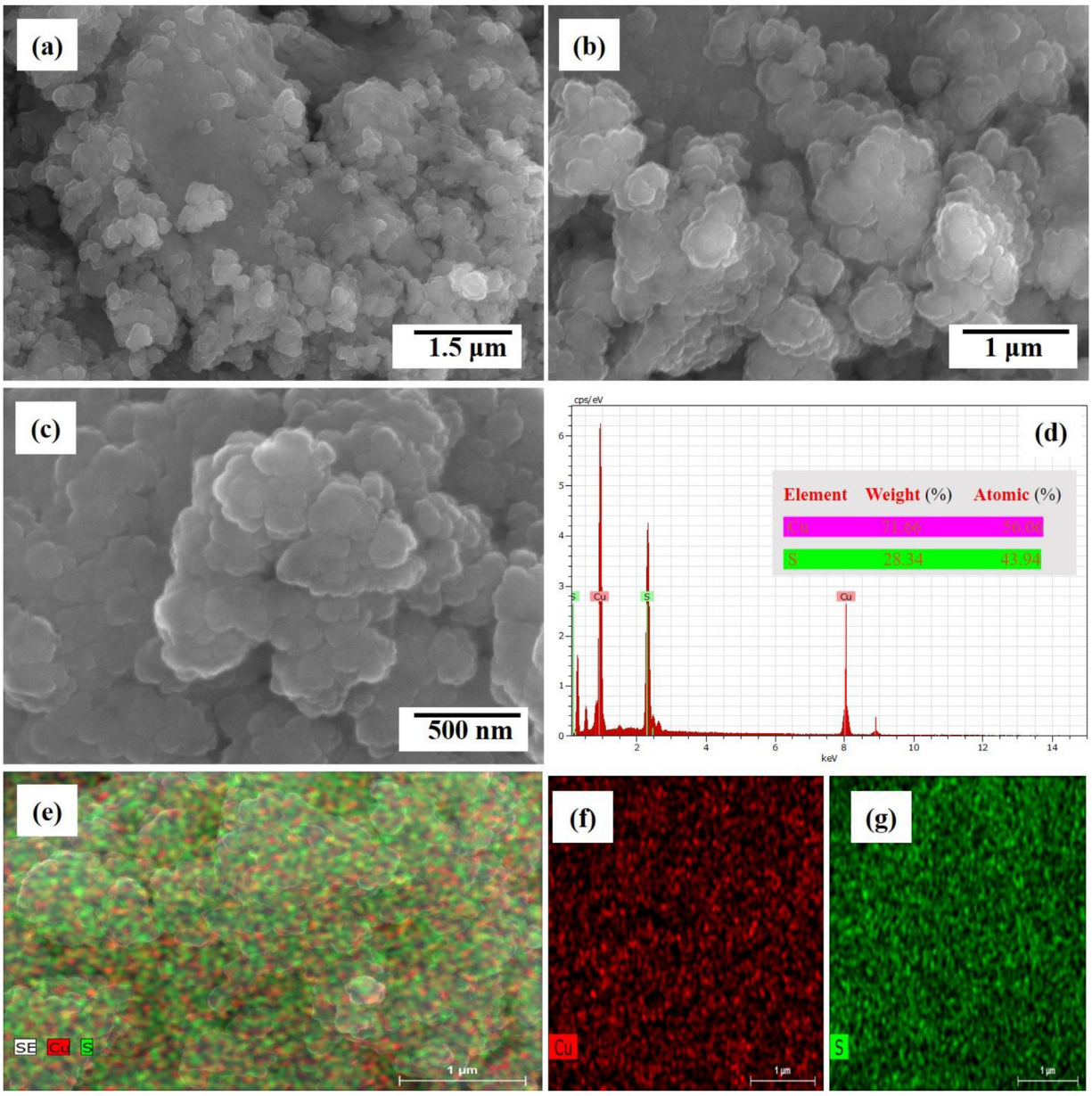

Fig. 4. FESEM images of CuS (a-c), EDX spectra (d) and Elemental mapping (e–g).

Table 1
Photodiode parameter of (a) p-CuS/n-Si, (b) p-CuO@CuS/n-Si (1:0.5), (c) p-CuO@CuS/n-Si (1:1) based diode such as Idealityfactor (n), Barrier height (Φ_B), Photosensitivity (P_S), Photoresponsivity (R), External Quantum efficiency (EQE)%, Specific detectivity (D*).

Diode Composition	Ideality factor n		Barrier height Φ_B (eV)		I_o (A)		Photo Sensitivity P_S (%)	Photo Responsivity R (mA/W)	Quantum Efficiency EQE (%)	Specific Detectivity D* (Jones)
	Dark	Light	Dark	Light	Dark	Light				
CuO	9.57	11.49	0.749	0.692	1.21×10^{-5}	1.09×10^{-4}	6.63×10^{3}	12.82	4.97	4.1×10^{10}
CuO/CuS (1:0.5)	8.84	7.18	0.664	0.631	3.48×10^{-4}	1.12×10^{-3}	1.00×10^{4}	581.23	225.37	3.39×10^{11}
CuO/CuS (1:1)	4.10	2.94	0.802	0.744	0.15×10^{-4}	0.14×10^{-3}	7.76×10^{4}	798.61	309.66	8.19×10^{11}

shorten peaks at 295, 333 cm^{-1} are corresponding to A_g mode and B_g mode of CuO formation respectively [40]. Similarly, high intensity Raman characteristic peaks are observed for CuO@CuS(1:1) nanoparticle corresponding to CuS (Fig. 3(c)), which explores that the high concentration of CuS particle over the surface of CuO of the core/shell formation. Characteristic peak at 473 cm^{-1} for both CuO@CuS (1:0.5) and CuO@CuS (1:1) samples, which is clearly red shifted when compared to bare CuS sample. The reason for the shifted peak may be raised at the junction of core-shell structure, because low ionic radii oxygen atoms replaced some of the high ionic radii sulfur site of CuS.

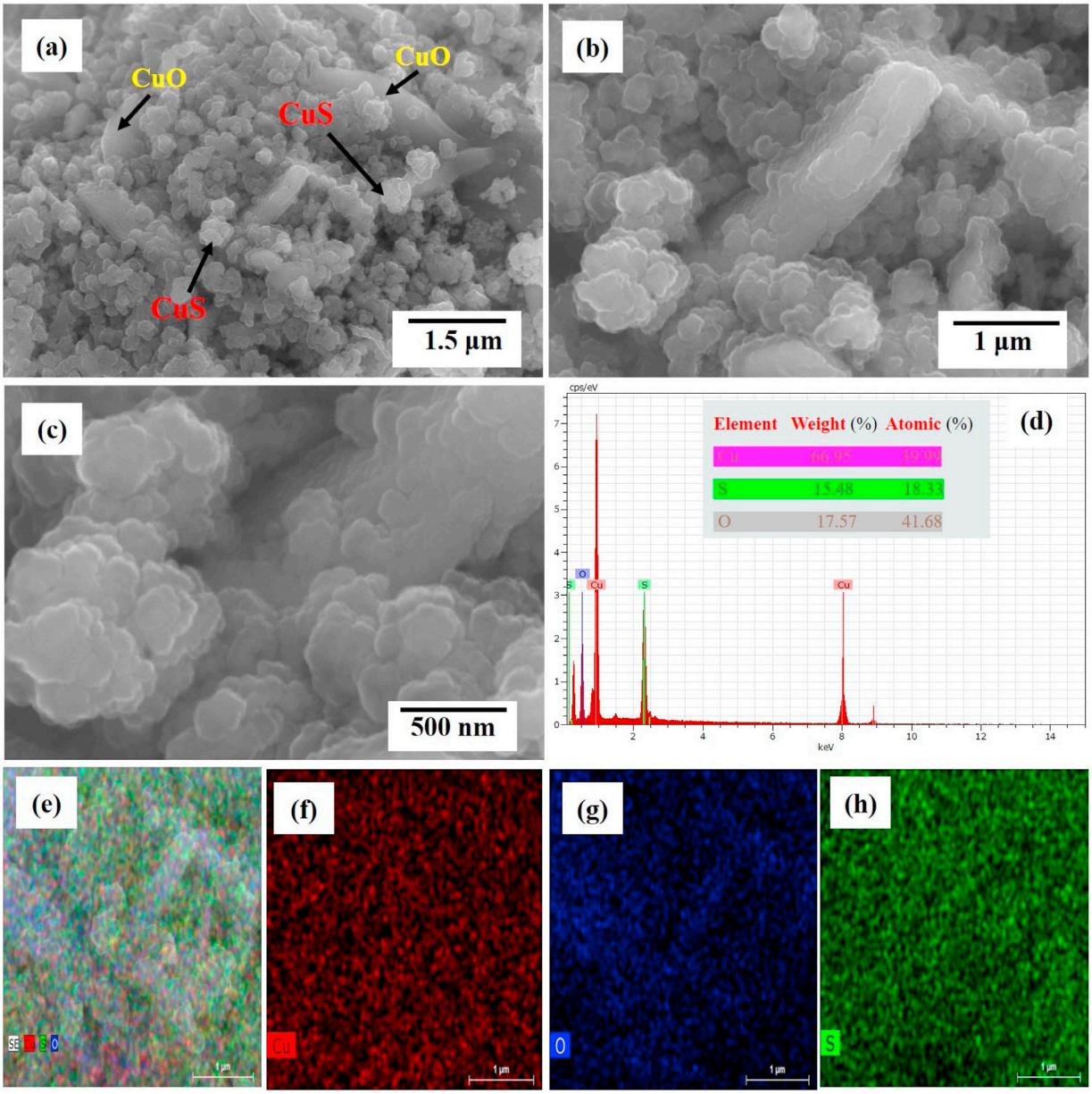

Fig. 5. FESEM images of CuO/CuS(1:0.5) (a–c), EDX spectra (d) and Elemental mapping (e–h).

Table 2
Comparison of the performance of various photodetectors with current one CuO@CuS.

Photodetectors	Photosensitivity P_s (%)	Photoresponsivity R	External quantum efficiency EQE (%)	Detectivity (Jones)	Target Wavelength	Reference
Ge/CdS	18,000	–	–	2.5×10^{10}	white light (1.9 mW cm^{-2})	[12]
p-CuO/n-MoS_2	–	—	–	3.27×10^{8} Jones	532 nm Laser Illumination	[14]
MoS_2(n)–CuO(p)	–	42 mA/W	–	–	554 and 780 nm	[17]
p-CuS-ZnS/n-ZnO		12 mA/W			300 nm	[23]
p-CuS-ZnS (p-CZS)	–	5.4 µA W^{-1}	–	1.6×10^{9} Jones	390 nm	[24]
p-CuO/n-ZnO	–	0.040 to 0.123 A/W	–	–	365 nm	[55]
MoS_2/Graphene	–	12.3 mA/W	–	1.8×10^{10}	532 nm Laser Illumination	[65]
ZnSe/ZnO	–	6.7 mA/W	–	4.1×10^{13}	365 nm	[66]
InS	58.58	0.598 mA/W		10.46×10^{7}	Visible light (100 mW/cm^2)	[67]
p-CuO@CuS/n-Si (1:1)	7.76×10^{4}	798.61 mA/W	309.66	8.19×10^{11}	Visible light (100 mW/cm^2)	Current work

3.3. FESEM analysis

The surface morphology of the synthesized pure CuS (Fig. 4), CuO@CuS (1:0.5) (Fig. 5) and CuO@CuS (1:1) (Fig. 6) was investigated by FE-SEM. In Fig. 4 (a–c), CuS particles were appeared as sphere like morphology and particles agglomeration may be due to physisorption of individual particles. It is clearly found that the size of particles is ~20 nm. EDX and elemental imaging of synthesized CuS were presented in Fig. 4 (d–g), which evident the presence of Cu and S elements. Fig. 5 (a–c) clearly indicates the formation

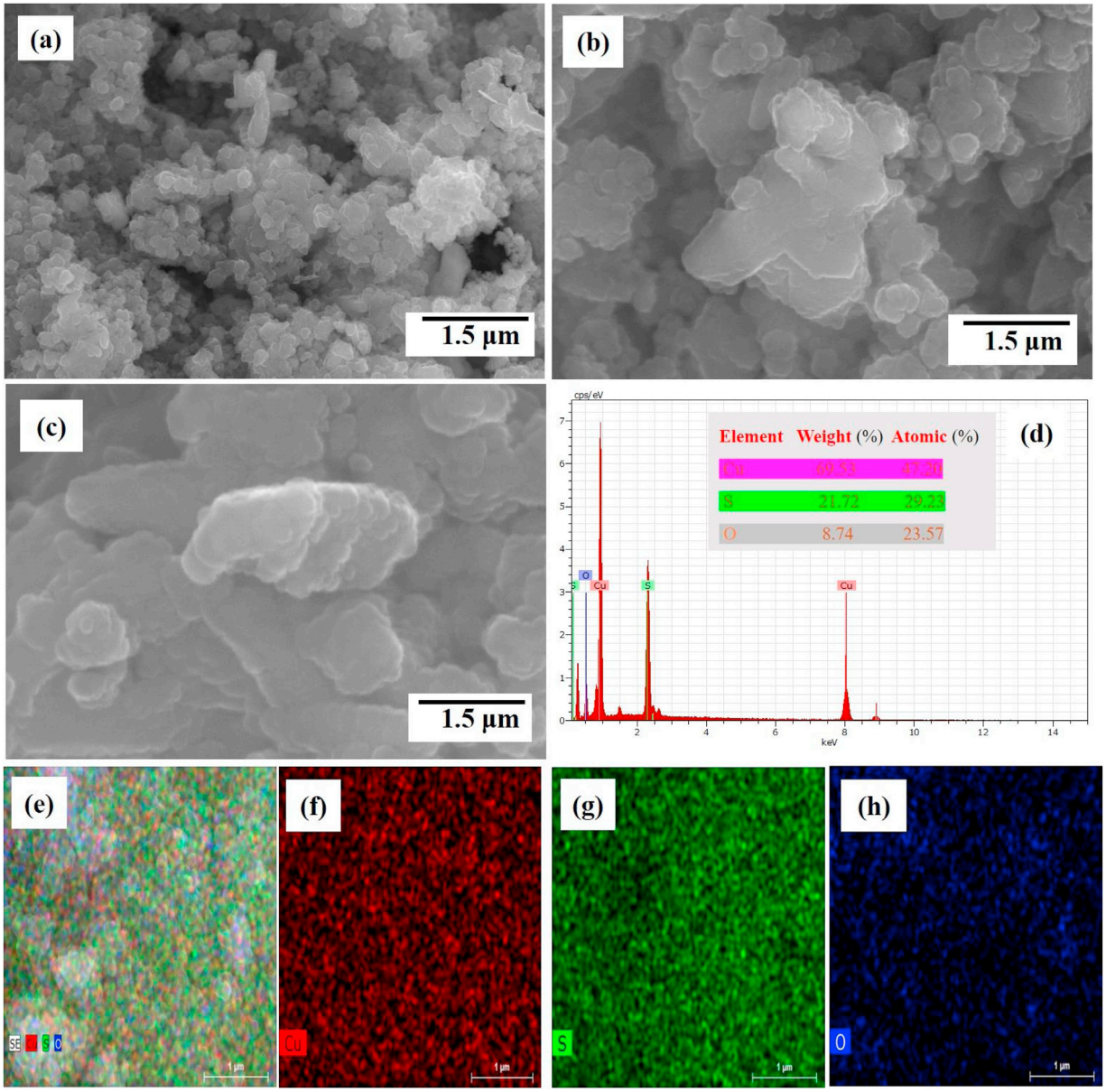

Fig. 6. FESEM images of CuO/CuS(1:1) (a–c), EDX spectra (d) and Elemental mapping (e–h).

CuO@CuS (1:0.5) particles. CuS nanospheres were spreaded over the CuO crossed sheets as core/shell structure. Lesser amount of CuS was used to construct CuO@CuS core/shell; core particles which are easily recognisable in the micrographs. EDX and elemental imaging of synthesized CuO@CuS(1:0.5) core/shell were presented in Fig. 5 (d–h), which revealed the percentage of Cu and S presence as 1:0.5 ratio and elemental mapping supports the above core/shell above results. FESEM micrographs of CuO@CuS (1:1) were presented in Fig. 6(a–c). CuS nanospheres were fully occupying the surface of the CuO nano crossed sheets. EDX and elemental imaging of synthesized CuO@CuS (1:1) core/shell systems are presented in Fig. 6 (d–h), which shows the percentage presence of Cu and S elements in (1:1) ratio. Remarkably, the plate like shapes was found because of CuO particles and CuS were randomly dispersed over plates as illustrated in Fig. 5 and 6. The reason could be the incorporation of different concentration of CuS to CuO gives a plate like shapes of metal oxide and metal sulphide spheres, respectively.

3.4. HRTEM analysis

TEM analysis was done for as synthesized CuO@CuS (1:1) Core@shell particles to understand the core/shell formation in detail and captured pictures were shown in Fig. 7(a–f). The micrographs Fig. 7 (a–c) clearly indicate that ~100 nm CuO sheets were surrounded by CuS particles, this approved the core/shell system formation. Fig. 7 (d–e) shows the HRTEM pictures of core@shell CuO@CuS. The crystal space distance was measured at 0.13 nm agreement with the CuO of (002) [41] and the adjacent interplanar spacing (0.191 nm) were measured in agreement with the CuS plane of (110) [42]. Interplanar spacing results confirms that the core is CuO and shell is CuS particles. The SAED pattern of CuO@CuS (1:1) Core@shell is shown in Fig. 7 (f) and confirms that the CuO@CuS nanoparticle appeared crystalline in nature.

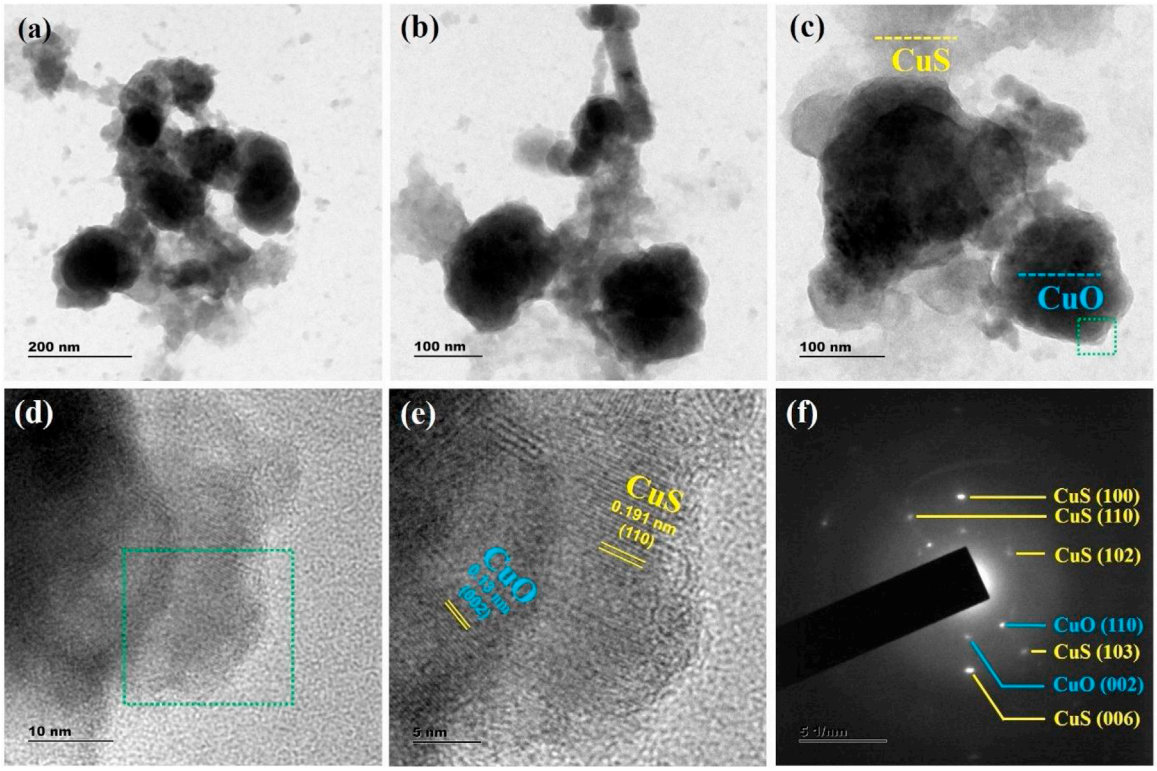

Fig. 7. HRTEM images of CuO/CuS(1:1) (a–c) lattice image (d–e) and SAED pattern (f).

3.5. I–V characterization of p-CuS/n-Si and p-CuO@CuS/n-Si diode

I–V curve of fabricated p-CuO@CuS/n-Si diodes with different level of CuS were shown in Fig. 8. The dark and photocurrent were measured in between the voltage range -3 and +3 V. The performance of the p-CuO@CuS/n-Si diode was examined by with and without light using portable solar simulator. From the Fig. 8, the photocurrent seems to very high under light condition which shows the better rectifying behaviour of the fabricated diodes. The current transport mechanism of p-CuO@CuS/n-Si diode was explained by the Thermionic Emission (TE) theory [43]:

$$I = I_0 \left[\exp\left(\frac{q(V - IR_s)}{nK_BT}\right) - 1\right] \quad (1)$$

where n is Ideality factor, K_B is Boltzmann constant, T is temperature in kelvin, R_s is series resistance, I_o is reverse saturation current and V is applied voltage. The reverse saturation current (I_o) calculated from the following equation [44].

$$I_o = AA^*T^2 \exp\left(-\frac{q\phi_B}{K_BT}\right) \quad (2)$$

here A is area of contact and A* is the Richardson constant, ϕ_B is zero bias barrier height. The dark current and photo current were found to be varied from 1.21 × 10^{-5} to 0.15 × 10^{-6} A and 1.09 ×10^{-4} to 0.14 × 10^{-3} A with CuS level. The high photo current of the diode is reflecting the surface modification of CuS sphere over the CuO nano-rod which reduce the trapping of charge carriers by surface absorption of oxygen. The same trend observed in ZnO-TiO_2 core/shell-based photo detector reported by Shao et. Al. [45]. The reverse saturation current (I_o) was improved from 10^{-5} to 10^{-3} due to the flow of minority charge carriers. The ideality factor (n) was calculated from the slop and intercepts of semi logarithmic plot (Fig. 9) using the following equation [46].

$$n = \frac{q}{k_BT}\frac{dV}{d(\ln J)} \quad (3)$$

The experimental values of n reduced from 11.49 to 2.94 with CuS level. For ideal diode, the n value should be unity (n = 1). Here, the n value of p-CuO@CuS/n-Si diode is greater than one which suggest the non-ideal behaviour of the fabricated diodes. The non-ideal behaviour of the diodes is mostly due to in homogeneity in the surface state, native oxide layer, diffusion current [47,48]. The decrease in ideality factor will enable the interface state to reduce the recombination of charge carriers in the junction [49]. The lower value of n under light condition for p-CuO@CuS (1:1)/n-Si evident that the decrease in recombination rate of electron hole pair at the junction, the similar result is reported by Mohan raj et al. [50]. The barrier height (Φ_B) for the fabricated device can be calculated by the following equation [51].

$$\Phi_B = \frac{K_BT}{q} \ln\left(\frac{AA^*T^2}{I_0}\right) \quad (4)$$

where A* is Richardson constant. The estimated value of barrier height was summarized in Table 1 which is varied between 0.631 to 0.802 eV. Under light condition, the obtained barrier height values are smaller than under dark condition exhibiting the more charge carrier which penetrates the higher barrier height to achieve conductivity [52]. The photosensitivity (P_S), responsivity (R), quantum efficiency (QE), specific directivity (D^*) are the vital parameters to investigate the photodiode/detector performance of the p-CuO@CuS/n-Si device. The photosensitivity (P_S) of the diode can be calculated from the following equation [53].

$$P_s(\%) = \frac{I_{Ph} - I_D}{I_D} \times 100 \quad (5)$$

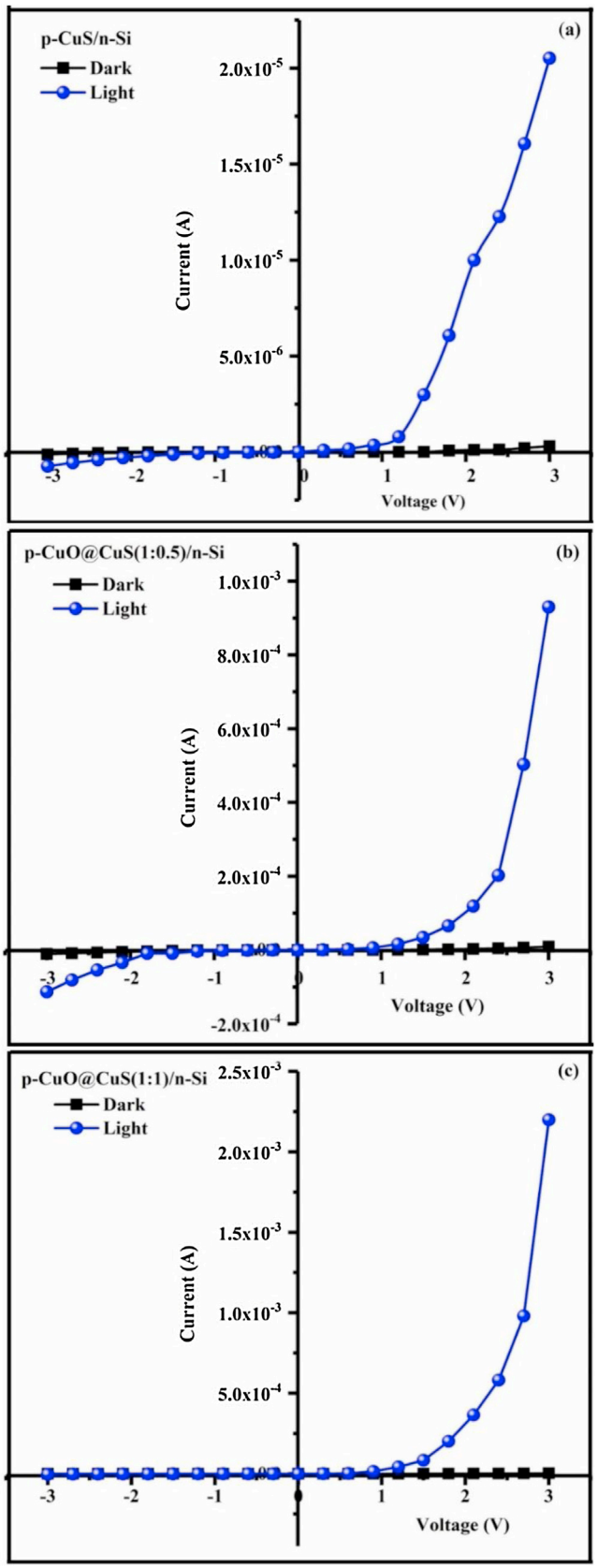

Fig. 8. I–V characteristics of (a) p-CuS/n-Si, (b) p-CuO@CuS/n-Si (1:0.5), (c) p-CuO@CuS/n-Si (1:1).

here I_{ph} and I_d are related to current under photo & dark environments. The photosensitivity of diode improved linearly with applied potential as shown in Fig. 10. The CuO@CuS(1:1)/n-Si diode reached a highest photosensitivity of 7.76 × 10^4 % at 3 V. The responsivity (R) was obtained from [54]:

$$R = \frac{I_{Ph}}{P \times S} \tag{6}$$

The estimated values of P_s, R, QE and D* for different systems are listed in Table 1. From Table 1, the responsivity was enhanced from 12. 82–798.61 mA/W while increasing CuS level. The maximum responsivity (R = 798.61 mA/W) is achieved for p-CuO@CuS(1:1)/n-Si diode which is 65 times higher than that of p-CuS/n-Si. Hence, the addition of Cu ions can effectively increase Ps of the p-CuS/n-Si diode. Resulting implies that the p-CuO@CuS (1:1)-n/Si is more adoptable for optoelectronic application. The R values of the currently developed p-CuO@CuS(1:1)/n-Si diode is higher than previously reported values for CuO or CuS core-shell based photodetectors like Wang et al. reported the nanostructured p-CuO/n-ZnO photodetector with responsivity ~ 0.040A/W at 1 V and 0.123 A/W at 2 V [55], Sahatiya et al. reported the MoS_2(n)–CuO(p) flexible diode with responsivity ~ 42 mA/W [17], Shin et al. developed the p-CuO/n-$Cu_{1-x}In_xO$ core/shell UV photodetector with responsivity ~ 0.045 A/W [18], Xu et al. p-CuS-ZnS/n-ZnO photodetectors with responsivity ~ 12 mA W^{-1} at 300 nm [23], Zhnag et al. developed the n-$SrTiO_3$ (n-STO) and p-CuS-ZnS (p-CZS) photodetectors with highest responsivity ~ 5.4 μA W^{-1} (at 390 nm), detectivity ~ 1.6 × 10^9 Jones [24], etc. These reports signify the current developed photodetectors is a good one as p-n junction.

The quantum efficiency is an additional factor used to analyse the performance of the device. The QE can be defined as the fraction of incident photons which contribute to the external photocurrent [56–58].

$$EQE = \frac{Rhc}{q\lambda} \tag{7}$$

here h is plank constant, c is light speed, R is responsivity, q is electron charge and λ is used light wavelength. The variations of QE with forward voltage and CuS levels are shown in Fig. 10. The p-CuO@CuS (1:1)-n/Si diode recorded a maximum QE of 309.66 % for 4 V. The increased lifetime of the photocarrier, superior creation of electron-hole and lower recombination are the reason for obtained maximum QE. The maximum outcome of quantum efficiency ensures the photo conducing nature of the present device. The specific detectivity is a key factor which is mostly influenced by dark current and it can be calculated from the following equation [59–62].

$$D^* = \frac{R S^{1/2}}{(2qI_D)^{1/2}} \tag{8}$$

The optimum signal detecting nature of detector is interrupted by noise produced in photodiode which is due to the thermal motion of charge carriers and electron hole pair recombination [63,64]. The detectivity is relatively low for the p-CuS/n-Si diode due to the large dark current and generation of weak photocurrent. The higher value of detectivity (D* = 8.19 × 10^{11} Jones) was noticed for p-CuO@CuS(1:1)/n-Si based diode which indicates that the lesser noise level of the device. The detectivity of the currently developed photodetector is better as well as comparable to earlier reported ones based on CuO and CuS core-shell photodetectors such as Zhang et al. reported p-CuO/n-MoS_2 with detectivity ~ 3.27 × 10^8 Jones [14], and Zhang et al. developed the n-$SrTiO_3$ (n-STO)

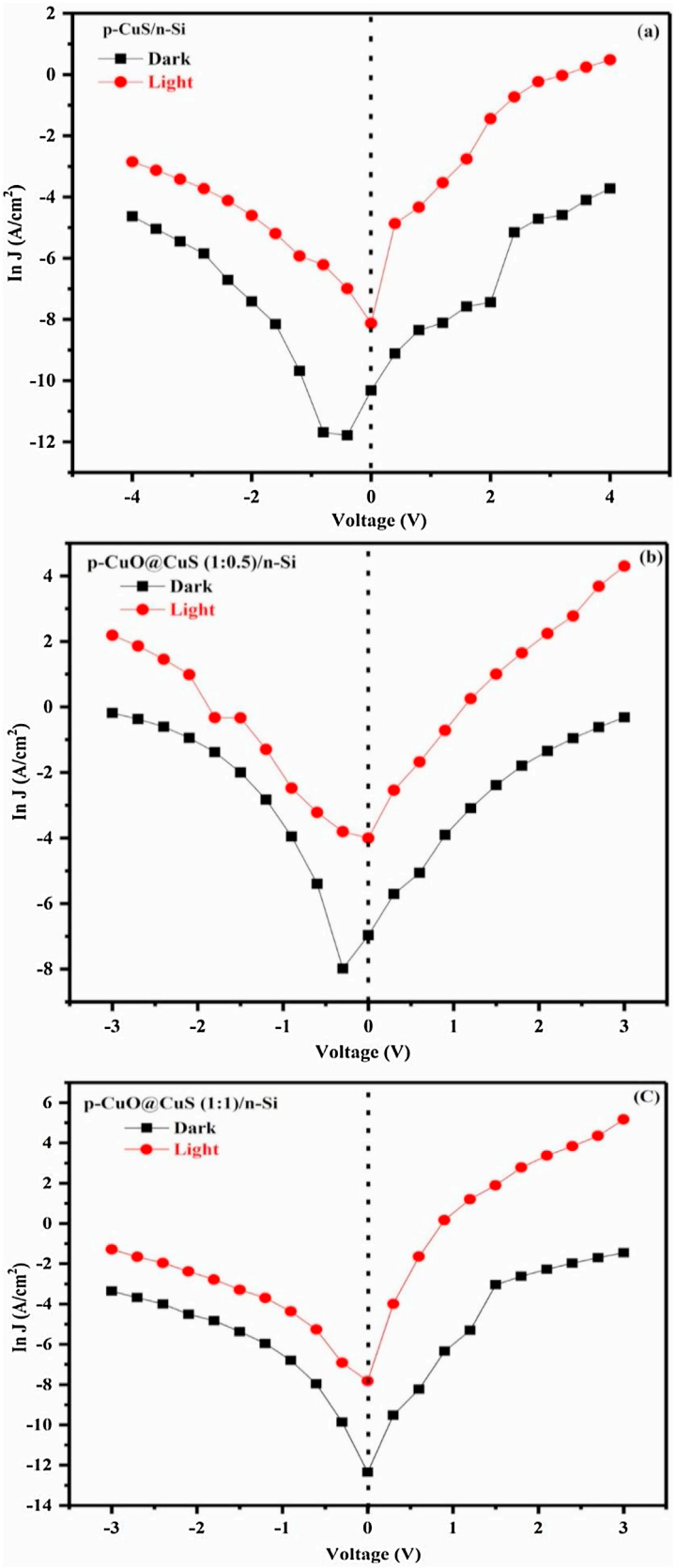

Fig. 9. Semi-logarithmic plot of ln (J) vsV of (a) p-CuS/n-Si, (b) p-CuO@CuS/n-Si (1:0.5), (c) p-CuO@CuS/n-Si (1:1).

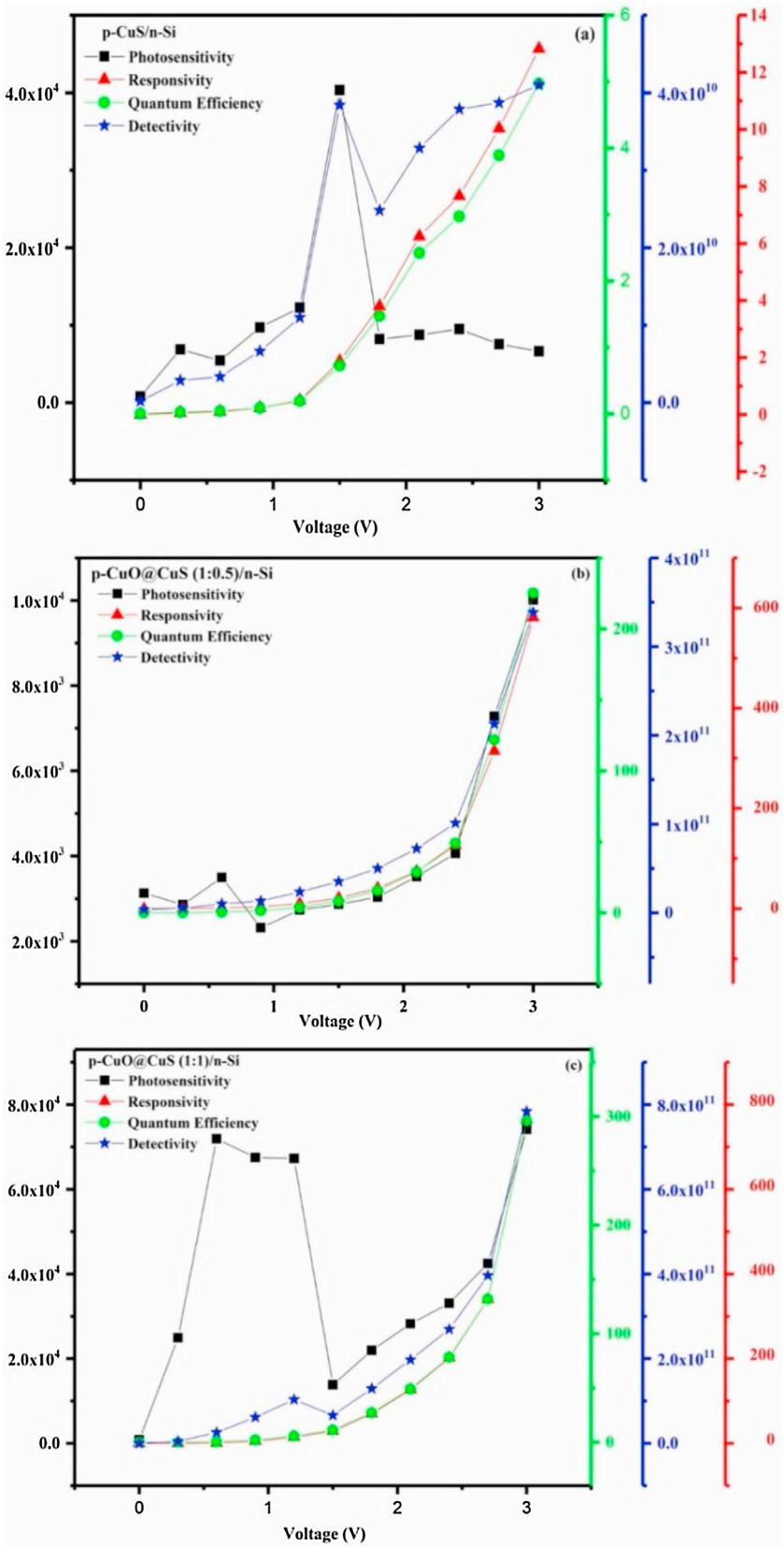

Fig. 10. Comparative plot of Ideality factor (n), Barrier height (Φ_B), Photosensitivity (P_S), Photoresponsivity (R), Quantum efficiency (QE)%, Specific detectivity (D^*) vs Voltage graph of (a) p-CuS/n-Si, (b) p-CuO@CuS/n-Si (1:0.5), (c) p-CuO@CuS/n-Si (1:1).

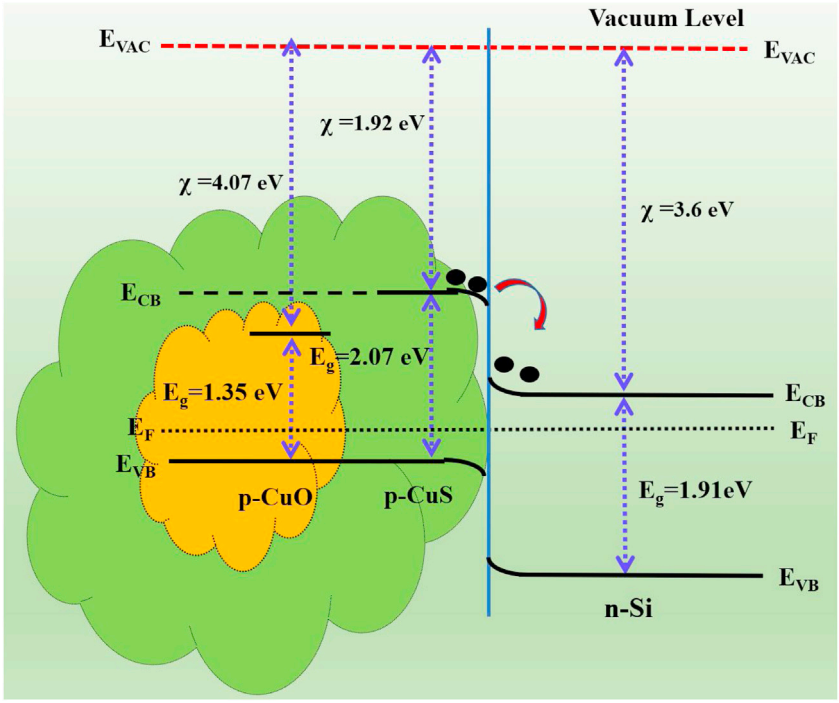

Fig. 11. Band diagram of p-CuO@CuS/n-Si diode.

and p-CuS-ZnS (p-CZS) photodetectors with detectivity ~ 1.6×10^9 Jones [24]. Possible band diagram of p-CuO@CuS/n-Si diode is presented in the Fig. 11. For more and better comparison, we have listed a number of reported photodetectors related values for developed photodetectors based on different type of materials in Table 2 [12,65–67].

4. Conclusion

In summary the CuS and core/shell CuO/CuS heterostructure were synthesized through chemical co-precipitation method. The XRD patterns were conforms the phase purity of samples which confirmed by the Raman analysis. SEM image confirms Sphere and Core/shell heterostructure of Pure CuS and CuO@CuS. The photodiodes are fabricated using satellite samples and diode behaviour are studied under dark and light condition. The highest photosensitivity (P_s) of 7.76×10^4 %, photoresponsivity (R) of 798.61 mA/W, maximum detectivity of $D^* = 8.19 \times 10^{11}$ Jones and EQE of 309.66 % were obtained for p-CuO@CuS (1:1)/n-Si diode. We observed the p-CuO@CuS (1:1)/n-Si diode will be highly suitable for photodetectors and can also be used in UV region.

Author agreement

The authors declares that:

The manuscript has not been previously published, is not currently submitted for review to any other journal, and will not be submitted elsewhere before a decision is made by this journal

Declaration of Competing Interest

Authors declares that there is no conflict of interest in current article.

Acknowledgements

The Author (D. Thangaraju) sincerely thank Science and Engineering Research Board (ECR/2017/002974), Department of Science and Technology, Government of India, for the financial support. The author from KKU would like to express his gratitude to RCAMS at King Khalid University, Saudi Arabia for sanctioning grant (RCAMS/KKU/009/19). The author T. Alshahrani extends her sincere appreciation to the Deanship of Scientific Research at Princess Nourah bint Abdulrahman University for funding this research through the Fast-track Research Funding Program.

References

[1] B. Pejjai, M. Reddivari, T.R.R. Kotte, Phase controllable synthesis of CuS nanoparticles by chemical co-precipitation method: effect of copper precursors on the properties of CuS, Mater. Chem. Phys. 239 (2020) 122030.
[2] M.S. Chavali, M.P. Nikolova, Metal oxide nanoparticles and their applications in nanotechnology, SN Appl. Sci. 1 (2019) 607.
[3] M. Balaji, J. Chandrasekaran, M. Raja, R. Marnadu, M. Ramamurthy, M. Shkir, Fabrication of ON/OFF switching response based on n-Ni-doped MoO_3/p-Si junction diodes using Ni-MoO_3 thin films as n-type layer prepared by JNS pyrolysis technique, Appl. Phys. A 126 (2020) 216.
[4] M. Raja, J. Chandrasekaran, M. Balaji, P. Kathirvel, R. Marnadu, Influence of metal (M = Cd, In, and Sn) dopants on the properties of spin-coated WO_3 thin films and fabrication of temperature-dependent heterojunction diodes, J. Solgel Sci. Technol. 93 (2020) 495–505.
[5] K.M. Chahrour, N.M. Ahmed, M.R. Hashim, A.M. Al-Diabat, High responsivity IR photodetector based on CuO nanorod Arrays/AAO assembly, Procedia Chem. 19 (2016) 311–318.
[6] X. Xu, S. Shukla, Y. Liu, B. Yue, J. Bullock, L. Su, et al., Solution-Processed Transparent Self-Powered p-CuS-ZnS/n-ZnO UV Photodiode, physica status solidi (RRL), Phys. Status Solidi Rapid Res. Lett. 12 (2018) 1700381.
[7] A. Costas, C. Florica, N. Preda, N. Apostol, A. Kuncser, A. Nitescu, et al., Radial heterojunction based on single ZnO-Cu x O core-shell nanowire for photodetector applications, Sci. Rep. 9 (2019) 1–9.
[8] F. Diao, Y. Wang, Transition metal oxide nanostructures: premeditated fabrication and applications in electronic and photonic devices, J. Mater. Sci. 53 (2018) 4334–4359.
[9] J. Tang, Z. Huo, S. Brittman, H. Gao, P. Yang, Solution-processed core–shell nanowires for efficient photovoltaic cells, Nat. Nanotechnol. 6 (2011) 568–572.
[10] S. Gunasekeran, D. Thangaraju, R. Marnadu, J. Chandrasekaran, T. Alshahrani, M. Shkir, et al., Fabrication of high-performance SiO_2@p-CuO/n-Si core-shell structure based photosensitive diode for photodetection application, Surf. Interfaces 20 (2020) 100622.
[11] V. Santhana, D.C. Greenidge, D. Thangaraju, R. Marnadu, T. Alshahrani, M. Shkir, Synthesis and emission characteristics of lead-free novel Cs_4SnBr_6/SiO_2 nanocomposite, Mater. Lett. (2020) 128562.

[12] Z. Sun, Z. Shao, X. Wu, T. Jiang, N. Zheng, J. Jie, High-sensitivity and self-driven photodetectors based on Ge–CdS core–shell heterojunction nanowires via atomic layer deposition, CrystEngComm 18 (2016) 3919–3924.
[13] D. Shao, M. Yu, H. Sun, T. Hu, J. lian, S. Sawyer, High responsivity, fast ultraviolet photodetector fabricated from ZnO nanoparticle–graphene core–shell structures, Nanoscale 5 (2013) 3664–3667.
[14] K. Zhang, M. Peng, W. Wu, J. Guo, G. Gao, Y. Liu, et al., A flexible p-CuO/n-MoS_2 heterojunction photodetector with enhanced photoresponse by the piezo-phototronic effect, Mater. Horiz. 4 (2017) 274–280.
[15] T. Xie, M.R. Hasan, B. Qiu, E.S. Arinze, N.V. Nguyen, A. Motayed, et al., High-performing visible-blind photodetectors based on SnO_2/CuO nanoheterojunctions, Appl. Phys. Lett. 107 (2015) 241108.
[16] W. Tian, C. Zhi, T. Zhai, X. Wang, M. Liao, S. Li, et al., Ultrahigh quantum efficiency of CuO nanoparticle decorated $In_2Ge_2O_7$ nanobelt deep-ultraviolet photodetectors, Nanoscale 4 (2012) 6318–6324.
[17] P. Sahatiya, S. Badhulika, Fabrication of a solution-processed, highly flexible few layer MoS_2 (n)–CuO (p) piezotronic diode on a paper substrate for an active analog frequency modulator and enhanced broadband photodetector, J. Mater. Chem. C 5 (2017) 11436–11447.
[18] D.S. Shin, I. Cho, T.G. Kim, S.H. Jeong, J. Park, Investigation of p-CuO/n-Cu1-xInxO core/shell nanowire structure performance in UV photodetectors, J. Alloys. Compd. 728 (2017) 1180–1185.
[19] S. Noothongkaew, O. Thumthan, K.-S. An, UV-Photodetectors based on CuO/ZnO nanocomposites, Mater. Lett. 233 (2018) 318–323.
[20] L.S. Vikas, K.C. Sanal, M.K. Jayaraj, A. Antony, J. Puigdollers, Vertically aligned ZnO nanorod array/CuO heterojunction for UV detector application, Phys. Status Solidi 211 (2014) 2493–2498.
[21] S. Mohammadi, M. Zavvari, High performance n-ZnO/p-metal-oxides UV detector grown in low-temperature aqueous solution bath, Thin Solid Films 626 (2017) 173–177.
[22] Y. Ji, U. Jung, Z. Xian, D. Kim, J. Yu, J. Park, Ultraviolet photodetectors using hollow p-CuO nanospheres/n-ZnO nanorods with a pn junction structure, Sens. Actuators A Phys. 304 (2020) 111876.
[23] X. Xu, S. Shukla, Y. Liu, B. Yue, J. Bullock, L. Su, et al., Solution-processed transparent self-powered p-CuS-ZnS/n-ZnO UV photodiode, Phys. Status Solidi RRL 12 (2018) 1700381.
[24] Y. Zhang, X. Xu, X. Fang, Tunable self-powered n-$SrTiO_3$ photodetectors based on varying CuS-ZnS nanocomposite film (p-CuZnS, p-CuS, and n-ZnS), InfoMat 1 (2019) 542–551.
[25] S. Panigrahi, D. Basak, Solution-processed novel core–shell n–p heterojunction and its ultrafast UV photodetection properties, RSC Adv. 2 (2012) 11963–11968.
[26] S. Li, Y. Zhang, W. Yang, H. Liu, X. Fang, 2D perovskite $Sr_2Nb_3O_{10}$ for high-performance UV photodetectors, Adv. Mater. 32 (2020) 1905443.
[27] Q. Zhang, X. Li, Z. He, M. Xu, C. Jin, X. Zhou, 2D semiconductors towards high-performance ultraviolet photodetection, J. Phys. D Appl. Phys. 52 (2019) 303002.
[28] H. Ying, X. Li, H. Wang, Y. Wang, X. Hu, J. Zhang, et al., Band structure engineering in MoS_2 based heterostructures toward high-performance phototransistors, Adv. Opt. Mater. 8 (2020) 2000430.
[29] X. Li, X. Xiong, Q. Zhang, Performance-enhancing ultraviolet photodetectors established on individual In_2O_3nanowires via coating a CuO layer, Mater. Res. Express 4 (2017) 045018.
[30] B. Liu, B. Tang, F. Lv, Y. Zeng, J. Liao, S. Wang, et al., Photodetector based on heterostructure of two-dimensional WSe_2/In_2Se_3, Nanotechnology 31 (2019) 065203.
[31] H.-J. Song, M.-H. Seo, K.-W. Choi, M.-S. Jo, J.-Y. Yoo, J.-B. Yoon, High-performance copper oxide visible-light photodetector via grain-structure model, Sci. Rep. 9 (2019) 1–10.
[32] Y.H. Ko, G. Nagaraju, S.H. Lee, J.S. Yu, Facile preparation and optoelectronic properties of CuO nanowires for violet light sensing, Mater. Lett. 117 (2014) 217–220.
[33] M. Raj, C. Joseph, M. Subramanian, V. Perumalsamy, V. Elayappan, Superior photoresponse MIS Schottky barrier diodes with nanoporous:Sn–WO_3 films for ultraviolet photodetector application, New J. Chem. 44 (2020) 7708–7718.
[34] S. Meghana, P. Kabra, S. Chakraborty, N. Padmavathy, Understanding the pathway of antibacterial activity of copper oxide nanoparticles, RSC Adv. 5 (2015) 12293–12299.
[35] M. Chandra, K. Bhunia, D. Pradhan, Controlled synthesis of CuS/TiO_2 heterostructured nanocomposites for enhanced photocatalytic hydrogen generation through water splitting, Inorg. Chem. 57 (2018) 4524–4533.
[36] T. Hurma, S. Kose, XRD Raman analysis and optical properties of CuS nanostructured film, Optik 127 (2016) 6000–6006.
[37] S. Adhikari, D. Sarkar, G. Madras, Hierarchical design of CuS architectures for visible light photocatalysis of 4-Chlorophenol, ACS Omega 2 (2017) 4009–4021.
[38] J. Kundu, S. Khilari, K. Bhunia, D. Pradhan, Ni-Doped CuS as an efficient electrocatalyst for the oxygen evolution reaction, Catal. Sci. Technol. 9 (2019) 406–417.
[39] M. Pal, N.R. Mathews, E. Sanchez-Mora, U. Pal, F. Paraguay-Delgado, X. Mathew, Synthesis of CuS nanoparticles by a wet chemical route and their photocatalytic activity, J. Nanoparticle Res. 17 (2015) 301.
[40] W. Wang, Q. Zhou, X. Fei, Y. He, P. Zhang, G. Zhang, et al., Synthesis of CuO nano- and micro-structures and their Raman spectroscopic studies, CrystEngComm 12 (2010) 2232–2237.
[41] A.T. Le, S.-Y. Pung, S. Sreekantan, A. Matsuda, D.P. Huynh, Mechanisms of removal of heavy metal ions by ZnO particles, Heliyon 5 (2019) e01440.
[42] Nu. Ain, R. Zia ur, A. Aamir, Y. Khan, M.-u. Rehman, D.-J. Lin, Catalytic and photocatalytic efficacy of hexagonal CuS nanoplates derived from copper(II) dithiocarbamate, Mater. Chem. Phys. 242 (2020) 122408.
[43] E. Uğurel, Ş. Aydoğan, K. Şerifoğlu, A. Türüt, Effect of 6 MeV electron irradiation on electrical characteristics of the Au/n-Si/Al Schottky diode, Microelectron. Eng. 85 (2008) 2299–2303.
[44] R. Marnadu, J. Chandrasekaran, S. Maruthamuthu, P. Vivek, V. Balasubramani, P. Balraju, Jet nebulizer sprayed WO_3-Nanoplate arrays for high-photoresponsivity based metal–Insulator–Semiconductor structured schottky barrier diodes, J. Inorg. Organomet. Polym. Mater. 30 (2020) 731–748.
[45] D. Shao, H. Sun, G. Xin, J. Lian, S. Sawyer, High quality ZnO–TiO_2 core–shell nanowires for efficient ultraviolet sensing, Appl. Surf. Sci. 314 (2014) 872–876.
[46] P. Vivek, J. Chandrasekaran, R. Marnadu, S. Maruthamuthu, V. Balasubramani, Incorporation of Ba2+ ions on the properties of MoO_3 thin films and fabrication of positive photo-response Cu/Ba–MoO_3/p-Si structured diodes, Superlattices Microstruct. 133 (2019) 106197.
[47] M. Balaji, J. Chandrasekaran, M. Raja, Characterization of $WMoO_3$ thin films and its n-$WMoO_3$/p-Si junction diodes via JNS pyrolysis technique, Z. Phys.Chem 231 (2017) 1017.
[48] N.M. Khusayfan, Electrical and photoresponse properties of Al/graphene oxide doped NiO nanocomposite/p-Si/Al photodiodes, J. Alloys. Compd. 666 (2016) 501–506.
[49] P. Sumathi, J. Chandrasekaran, R. Marnadu, S. Muthukrishnan, S. Maruthamuthu, Synthesis and characterization of tungsten disulfide thin films by spray pyrolysis technique for n-WS_2/p-Si junction diode application, J. Mater. Sci. Mater. Electron. 29 (2018) 16815–16823.
[50] K. Mohanraj, D. Balasubramanian, K. Porkumaran, N. Jhansi, J. Chandrasekaran, Impact of Ce content on cubic phase cerium–cadmium oxide (Ce–CdO) nanoparticles and its n-CeCdO/p-Si junction diodes, J. Mater. Sci. Mater. Electron. 29 (2018) 20439–20454.
[51] M. Balaji, J. Chandrasekaran, M. Raja, Role of substrate temperature on MoO_3 thin films by the JNS pyrolysis technique for P–N junction diode application, Mater. Sci. Semicond. Process. 43 (2016) 104–113.
[52] A. Özmen, S. Aydogan, M. Yilmaz, Fabrication of spray derived nanostructured n-ZnO/p-Si heterojunction diode and investigation of its response to dark and light, Ceram. Int. 45 (2019) 14794–14805.
[53] D. Thangaraju, R. Marnadu, V. Santhana, A. Durairajan, P. Kathirvel, J. Chandrasekaran, et al., Solvent influenced synthesis of single-phase SnS_2 nanosheets for solution-processed photodiode fabrication, CrystEngComm 22 (2020) 525–533.
[54] G. Liu, Z. Li, X. Chen, W. Zheng, W. Feng, M. Dai, et al., Non-planar vertical photodetectors based on free standing two-dimensional SnS_2 nanosheets, Nanoscale 9 (2017) 9167–9174.
[55] S. Wang, C. Hsiao, S. Chang, Z.Y. Jiao, S. Young, S. Hung, et al., ZnO branched nanowires and the p-CuO/n-ZnO heterojunction nanostructured photodetector, IEEE Trans. Nanotechnol. 12 (2013) 263–269.
[56] C. Li, W. Huang, L. Gao, H. Wang, L. Hu, T. Chen, et al., Recent advances in solution-processed photodetectors based on inorganic and hybrid photo-active materials, Nanoscale 12 (2020) 2201–2227.
[57] M. Shkir, M.T. Khan, I.M. Ashraf, A. Almohammedi, E. Dieguez, S. AlFaify, High-performance visible light photodetectors based on inorganic CZT and InCZT single crystals, Sci. Rep. 9 (2019) 12436.
[58] M. Shkir, I.M. Ashraf, K.V. Chandekar, I.S. Yahia, A. Khan, H. Algarni, et al., A significant enhancement in visible-light photodetection properties of chemical spray pyrolysis fabricated CdS thin films by novel Eu doping concentrations, Sens. Actuators A Phys. 301 (2020) 111749.
[59] R. Chai, Z. Lou, G. Shen, Highly flexible self-powered photodetectors based on core–shell Sb/CdS nanowires, J. Mater. Chem. C 7 (2019) 4581–4586.
[60] M. Shkir, I.M. Ashraf, A. Khan, M.T. Khan, A.M. El-Toni, S. AlFaify, A facile spray pyrolysis fabrication of Sm:CdS thin films for high-performance photodetector applications, Sens. Actuators A Phys. 306 (2020) 111952.
[61] S. Mohd, I.M. Ashraf, S. AlFaify, Surface area, optical and electrical studies on PbS nanosheets for visible light photo-detector application, Phys. Scr. 94 (2019) 025801.
[62] M. Shkir, I. Ashraf, S. AlFaify, A.M. El-Toni, M. Ahmed, A. Khan, A noticeable effect of Pr doping on key optoelectrical properties of CdS thin films prepared using spray pyrolysis technique for high-performance photodetector applications, Ceram. Int. 46 (2020) 4652–4663.
[63] Y. Guo, Y. Li, Q. Zhang, H. Wang, Self-powered multifunctional UV and IR photodetector as an artificial electronic eye, J. Mater. Chem. C 5 (2017) 1436–1442.
[64] A.K. Katiyar, A.K. Sinha, S. Manna, R. Aluguri, S.K. Ray, Optical photoresponse of CuS–n-Si radial heterojunction with Si nanocone arrays fabricated by chemical etching, J. Chem. Soc. Faraday Trans. 15 (2013) 20887–20893.
[65] H. Xu, X. Han, X. Dai, W. Liu, J. Wu, J. Zhu, et al., High detectivity and transparent few-layer MoS_2/glassy-graphene heterostructure photodetectors, Adv. Mater. 30 (2018) 1706561.
[66] X. Zhang, D. Hu, Z. Tang, D. Ma, Construction of ZnSe–ZnO axial p–n junctions via regioselective oxidation process and their photo-detection applications, Appl. Surf. Sci. 357 (2015) 1939–1943.
[67] H. Kumar, S. Kumar, Indium sulfide based metal-semiconductor-metal ultraviolet-visible photodetector, Sens. Actuators A Phys. 299 (2019) 111643.

Biographies

S. Gunasekaran received his M.Sc. degree from Bharathidasan university, India in 2016. He is currently working towards Ph.D. degree in the department of physics in PSG College of Arts and Science, India, His current research interest is nanoparticle synthesis and optoelectronic device applications.

Dr. D. Thangaraju received his Ph.D., from Crystal Growth Centre, Anna university Chennai, India in 2012. He has done his post-doctoral research at ChimieParisTech, France (2012–13) and JSPS post-doctoral research at Shizuoka University, Japan (2014–16) on fabrication of multifunctional nano structures. He is currently working as Assistant Professor at Department of Physics, PSG Institute of Technology and Applied Research in Coimbatore, India. His current research under nano–crystal Design and Application Lab (n-DAL), includes, nano crystal growth, optoelectronic devices fabrication, nanobiotechnology, and bioimaging.

R. Marnadu has received his B.Sc. degree in Physics from Madurai Kamaraj University, Madurai (India) and M.Sc. in Physics from Bharathiar University, Coimbatore (India). Currently he is pursuing Ph.D. in Physics at Department of Physics, Sri Ramakrishna Mission Vidyalaya College of arts and science, Coimbatore (India) with specialization in Material Science. His research interest focuses on the development of low-cost UV photodetector, MIS type Schottky structure, photo-diode, and thin film based semiconductor devices for optoelectronic application.

Dr. J. Chandrasekaran received his BS and MS degrees and Doctor of Philosophy in Physics from Madurai Kamaraj University, Madurai (India), He Currently working as Associate Professor and Head, Department of Physics, Sri Ramakrishna Mission Vidyalaya College of Arts & Science, Coimbatore India (Oct 1988 – Till date). His current research interests include Fabrication of Electronic Devices especially Solar Cell, semiconductor diodes and NLO Material Characterization

Dr. Mohd. Shkir: Currently he is an Assistant Professor, at department of Physics, King Khalid University, Abha, Saudi Arabia. He has published over 330 research papers in high impact international and national journals with over 5005 citations, h-index-37, i10-index 163 and also published one patent [ES2527976 (A1) — 2015–02-02]. He is leading a research group "Investigation on Novel Class of Materials (INCM) at KKU". He was born in Pilibhit, UP, India in 1982. He received his B.S. and M.S. in Physics from M.J.P. Rohilkhand University (MJPRU), Bareilly, India. He received his Doctor of Philosophy (Ph.D.) from Jamia Millia Islamia (a central university), India. Very recently he receives an Excellenec award named "Dr. Sulaiman Al Habib Award for Excellenec in Scientific Research 2020" for working on a project "Structure-based modulation of SARS-CoV2 Nucleocapsid protein-protein interaction: Towards drug designing against COVID-19" (COVID-19 RC#09). He got DS Kothari Post-Doctoral fellowship award and research associate from Solar Energy Centre: Government of India, He did his post-doctoral (PDF) research from Crystal Growth Lab (CGL), Universidad Autónoma de Madrid (UAM), Madrid, Spain with Prof. E. Diegues, on topic of "System for Manufacturing Solar Cells For Multilayer And Procedure For Making These" and have patent on it. He worked in University of Delhi (DU) and Manav Rachna College of engineering (MRCE) as an Assistant Professor of Physics. He also confirmed to receive IAAM Young Scientist Medal 2018, Singapore. He also gets nominated for "Researchers' Award for Revolutionary Findings', by Maharshi Dayanand Saraswati University, India. His scientific interest focused on nonlinear optics, nanotechnology and thin film fabrications for optoelectronic device applications which combines experimental and theoretical techniques. Fabrication of new systems and devices for future applications. He is working on determination of various electro-optical properties using computational techniques. He is currently working on Nano-synthesis of different kind of materials for biomedical, optoelectronic and radiation detection applications.

Dr. Durairajan Arulmozhi is currently a postdoctoral researcher in the Institute of Nanostructures, Nanomodeling and Nanofabrication (I3N), Department of Physics, University of Aveiro (UA), Aveiro, Portugal. He received his bachelor, master and Doctorate degrees in Physics from Thiruvalluvar University, Madurai Kamraj University and Anna University, India, in 2006, 2008 and 2015, respectively. His research is focused on the oxide nanomaterials, single crystals and thin films, with a focus on their dielectric, magnetic, and optical functionalities.

Dr. M.A. Valente is currently working as a associate professor in the Institute of Nanostructures, Nanomodeling and Nanofabrication (I3N), Department of Physics, University of Aveiro (UA), Aveiro, Portugal. He received his Ph.D. degree from same institution. Then, he joined the Department of Physics, University of Aveiro as an Assistant Professor. His research focuses on dielectric, ferroelectric, piezoelectric, and multiferroic properties of glass, glass ceramics, nanomaterials, single crystals and thin films.

Dr. M. Elango received his Ph.D. from Anna university, Chennai in 2013. He is currently working as Assistant Professor in Department of Physics, PSG College of Arts and Science in India. His current research interest includes nanomaterials, thin film, and optoelectronic devices application. He has authored and co-authored more than 15 articles on international journals including Surfaces and Interfaces, Materials Science in Semiconductor Processing, Journal of Alloys and Compounds and so on.